A force field of Li$^+$, Na$^+$, K$^+$, Mg^{2+}, Ca^{2+}, Cl$^-$, and SO_4^{2-} in aqueous solution based on the TIP4P/2005 water model and scaled charges for the ions

I. M. Zeron (iD), J. L. F. Abascal (iD), and C. Vega (iD)

View Online   Export Citation   CrossMark

ARTICLES YOU MAY BE INTERESTED IN

A force field of Li$^+$, Na$^+$, K$^+$, Mg^{2+}, Ca^{2+}, Cl$^-$, and SO$_4^{2-}$ in aqueous solution based on the TIP4P/2005 water model and scaled charges for the ions

I. M. Zeron, [ID] J. L. F. Abascal, [ID] and C. Vega[a] [ID]

AFFILIATIONS

Depto. Química Física, Fac. Ciencias Químicas, Universidad Complutense de Madrid, 28040 Madrid, Spain

[a]cvega@quim.ucm.es

ABSTRACT

In this work, a force field for several ions in water is proposed. In particular, we consider the cations Li$^+$, Na$^+$, K$^+$, Mg^{2+}, and Ca^{2+} and the anions Cl$^-$ and SO$_4^{2-}$. These ions were selected as they appear in the composition of seawater, and they are also found in biological systems. The force field proposed (denoted as Madrid-2019) is nonpolarizable, and both water molecules and sulfate anions are rigid. For water, we use the TIP4P/2005 model. The main idea behind this work is to further explore the possibility of using scaled charges for describing ionic solutions. Monovalent and divalent ions are modeled using charges of 0.85 and 1.7, respectively (in electron units). The model allows a very accurate description of the densities of the solutions up to high concentrations. It also gives good predictions of viscosities up to 3 m concentrations. Calculated structural properties are also in reasonable agreement with the experiment. We have checked that no crystallization occurred in the simulations at concentrations similar to the solubility limit. A test for ternary mixtures shows that the force field provides excellent performance at an affordable computer cost. In summary, the use of scaled charges, which could be regarded as an effective and simple way of accounting for polarization (at least to a certain extend), improves the overall description of ionic systems in water. However, for purely ionic systems, scaled charges will not adequately describe neither the solid nor the melt.

I. INTRODUCTION

On Earth, the overwhelming majority of water is found in oceans and seas. For this reason, more often than not, samples of water always contain a certain amount of solved salts. Since life started in the oceans, it is not surprising that many of the ions present in the seas are also found in the living cells, although at lower concentrations. For this reason, it is clear that understanding ionic solutions is of fundamental interest in, at least, two important systems: oceans and living organisms. For these systems, the typical conditions of interest are not too far away from the room temperature and room pressure (or for moderate pressures up to 1400 bars in deep water). However, the composition often changes from one system to another. For this reason, it is not possible to have experimental measurements of ionic solutions for a wide range of pressures, temperatures, and compositions. Computer simulations could be useful to predict some of the properties and to understand the outcome of the experimental measurements.

In computer simulations, the key factor controlling the accuracy of the predictions is the form of the intermolecular potential between the different species. This is usually denoted as the force field. In the 1970s and 1980s, it was common to model ionic solutions using an implicit description of water. In this description, water was not included in the simulations, but rather its presence was taken into an implicit way by scaling the coulombic interactions between ions by the dielectric constant of water. Certainly, in this treatment, simulations were quite fast since water is the most abundant component in ionic solutions. This approach may be justified at very low concentrations when the ions are quite far apart, but it will not work for moderate or high concentrations when the ions are closer. With the increase in computer power, the simulation of ionic systems using atomistic models of water became more popular in the last 30 years.

Until recently, force fields for ionic solutions in water were mainly designed to reproduce experimental values of the hydration free energies and the first peak of the radial distribution functions (RDFs). In some cases, the lattice energies of the ionic crystal or quantum-mechanical data on ion-water clusters in the gas-phase were also taken into account. Polarizable and nonpolarizable force fields have been proposed in the literature for alkali and alkaline earth halides.[1–28] Quite often, the force fields are based on nonpolarizable water models as SPC,[29] SPC/E,[30] TIP3P,[31] TIP4P,[31] TIP4P-Ew,[32] and TIP4P/2005,[33] but there are also polarizable models as POL1,[34] RPOL,[35] SWM4-DP,[36,37] and B3K.[38] An overview of the force fields available up to 2011 can be found in Table I of the paper by Reif and Hünenberger,[19] and a set of possible target properties to be used for the validation of potential parameters is shown in Fig. 5 of the cited reference. A more recent review by Nezbeda et al.,[39] focused on aqueous sodium chloride, discusses in detail the importance of the training set properties used to fit the force field parameters.

The need of a broader check of the properties of these model systems was clearly underlined by Joung and Cheatham.[15] These authors reported the formation of salt crystals well below the experimental saturation limit in simulations of alkali halide aqueous solutions using different force fields. In fact, precipitation in NaCl,[13,40–43] KCl,[15,44] CaCl$_2$,[45] Na$_2$SO$_4$,[46] and Li$_2$SO$_4$[47] at concentrations below the solubility limit has been reported in simulation studies. Joung and Cheatham also provided some examples indicating that the anomalous crystallization had lead in fact to erroneous interpretations of the results of some previous computer simulations. It is thus important to ensure that the force field has a solubility limit as close as possible to the experimental value.

Unfortunately, the calculation of the solubility by computer simulation is not a trivial task. It started in 2002 with the pioneering contribution of Ferrario et al.[48] who calculated the solubility limit of KF in water. In 2007, Sanz and Vega[49] evaluated the solubility of NaCl. Other groups continued these calculations.[50–54] After some initial discrepancies, a final agreement[26,54,55] was found for two common force fields for NaCl in water, namely, the Smith-Dang[7] and the Joung-Cheatham models (both in SPC/E water). The solubility was 0.7 m and 3.7 m, respectively, to be compared with the experimental result of 6.1 m. Since the nucleation of crystallites is an activated process, the spontaneous precipitation is only observed at concentrations 4–5 times larger than the solubility limit. This fact, which could be viewed as an advantage, may also hide important inaccuracies of the force field.

In 2012, Kim et al.[56] pointed out that none of the tested rigid, nonpolarizable models was able to reproduce the experimental trend for the concentration dependence of the diffusion coefficient of water in electrolyte solutions. Some of them even change the sign of the slope of the curves. They concluded that the form of the interaction potentials had to be reexamined. Similar conclusions were reached by Kann and Skinner.[57] Also recently, it has been possible to determine activity coefficients for salts in water.[58] It has been shown that the activity coefficient of salt increases too quickly with concentration. Due to the Gibbs-Duhem relation, this also means that the activity of water decreases too quickly—as compared to the experiment—with the concentration of the salt. Since the activity of water controls all the colligative properties, one cannot expect a good description of properties such as cryoscopic descent, osmotic pressure, and vapor pressures of salts solutions.

After these facts, the scenario looks rather depressive. Moreover, if the situation of monovalent electrolytes is already bad, that of divalent ions such as Mg^{2+}, Ca^{2+}, and SO$_4^{2-}$ are even worse. Everything seems to point out that the inclusion of polarization is needed to describe ions in water. Note that developing a good polarizable force field is not an easy task. If not parameterized with care, sometimes a bad polarizable force field yields worse results than a properly optimized nonpolarizable one. Since 2009, Leontyev and Stuchebrukhov[59–64] published a series of papers that brought the last opportunity to nonpolarizable force fields for ionic aqueous solutions. They proposed that maybe the charge of the ions should not be an integer number (in electron units) and that a scaled value should be used. They argued that nonpolarizable models do not fully account for the electronic contribution to the dielectric constant and proposed that the screening effect of the electronic continuum could be effectively included by a simple scaling of the charges, namely, $q_{scaled} = q/\sqrt{\varepsilon_{el}}$, where ε_{el} is the high frequency dielectric constant of water. This would lead to a scaled charge for monovalent ions of about 0.75. The use of scaled charges may find its justification as coming from the charge transfer and/or polarization of the water molecules around an ion.[65]

The first paper of Leontyev and Stuchebrukhov in this line was not received with enthusiasm at the beginning. After all, for a chemist, it is difficult to accept scaled charges since the unscaled values have provided excellent results for ionic crystals. Jungwirth was probably the first to advocate this idea.[45,47,66–68] Kann and Skinner[57] revisited the challenge of Kim et al.[56] and concluded that the scaling of the charges improved the description of the dynamical properties. Similarly, Yao et al.[65] have shown that the inclusion of dynamical charge transfer among water molecules accounts for the distinct behavior of the water diffusivity in NaCl(aq) and KCl(aq). In the same spirit, we have recently argued that the charges used in computer simulations describe the potential energy surface rather than the dipole moment surface (DMS),[69] an idea that has been further expanded by Jorge and co-workers.[70,71] Even ourselves, after one year of efforts trying to optimize a model for NaCl using unit charges for the ions, adopted the proposal of Leontyev and Stuchebrukhov because of a simple argument: it seems to work. We thus proposed a model for sodium chloride solutions, denoted as the Madrid model,[72] using $q_{scaled} = 0.85$. Recently, in a study of the surface of a NaCl solution in water, Škvára and Nezbeda have shown that the results of the nonpolarizable Madrid model and the polarizable AH/BK3 model[25] are found in most cases in mutual agreement.[73] Other work implementing the idea of charge scaling for electrolytes in water is that of Fuentes-Azcatl and Barbosa[74] who proposed a force field for NaCl using $q_{scaled} = 0.885$. Li and Wang[75,76] have also applied the charge scaling concept to monovalent ions using $q_{scaled} = 0.804$. In summary, the number of groups following the suggestion of Leontyev and Stuchebrukhov is growing in recent years (see also Refs. 77 and 78).

Although it is clear that the description of ions in water may improve when polarization is included, it seems of interest to probe nonpolarizable force fields using scaled charges. It is obvious that the scaling will have some limitations, but it maybe convenient to explore its limits before going to the polarizable models. The goal

of this work is to develop a force field for ionic solutions in water based on the use of scaled charges for the ions. Since the performance of a force field for ions in water is related to the performance of the model chosen to represent the water interactions, it is essential to employ a satisfactory force field for water. In such a case, good predictions of the solution properties will also be obtained at the infinite dilution limit. Among the rigid nonpolarizable water models, we have chosen[33] TIP4P/2005, which provides an excellent description of a number of properties of liquid and solid water.[79,80] For monovalent ions, we use a scaled value of the charge, in particular, 0.85 (in electron units). This was our optimized value of the ionic charges in a recently developed model for NaCl in TIP4P/2005 water which is able to describe the NaCl aqueous solution quite accurately.

Here, we extend the idea to other ions. The species selected in this work are essentially those typically found in seawater and biological fluids. In particular, we will consider the monovalent cations Na$^+$ and K$^+$ (as well as Li$^+$) and the divalent cations Mg^{2+} and Ca^{2+}. For consistency, the scaled charges would be 1.7 in the latter case. With regard to anions, the most interesting ones seem to be Cl$^-$ and SO$_4^{2-}$. The proposed force field is transferable in the sense that the water-ion and ion-ion interactions would be the same regardless of the composition of the system. In other words, the Cl–Cl or Cl–water interactions would be the same in NaCl, KCl, MgCl$_2$, or CaCl$_2$ aqueous solutions so that the force field could be used for any type of mixture.

The force field proposed in this work will be denoted as the Madrid-2019 force field. The target properties used to develop the force field were the solution densities, radial distribution functions, hydration numbers, and densities related to those of the melt and of the solid (see discussion below). Solubility was not directly used as a target property. The main reason is that it has become clear recently that the use of the scaling of the charges does not lead to good estimates of the nucleation rate for salt crystallization.[81] One should recognize from the very beginning that the scaling prevents an accurate description of the solid phase and/or the molten salts. The lack of transferability to other phases is the price to pay to improve the description of the solutions. We have taken into account solubility in an indirect way. We have checked that no spontaneous precipitation is observed at the experimental solubility limit after long simulation runs in large systems. We have also checked that the number of contact ion pairs (CIP) was always relatively low as we have recently shown that these figures should not be too high at the solubility limit.[82] Thus, even though we cannot guarantee that the proposed force field will reproduce the experimental values of the solubility limits, we can at least guarantee that the system will not precipitate at these concentrations, which otherwise would certainly invalidate the outcome of the simulations. We shall present results not only for pure salt solutions but also for several ternary mixtures showing that the predictions are also quite reasonable for these independent test systems.

II. THE MADRID 2019 FORCE FIELD

We assume that the total energy of the system is given by the sum of the potential energy between the molecules/ions of the system (pairwise approximation). The interaction between any pair of atoms i, j of the system is given by a coulombic term plus a Lennard-Jones (LJ) potential,

$$V(r_{ij}) = \frac{1}{4\pi\varepsilon_0} \frac{q_i q_j}{r_{ij}} + 4\epsilon_{ij}\left[\left(\frac{\sigma_{ij}}{r_{ij}}\right)^{12} - \left(\frac{\sigma_{ij}}{r_{ij}}\right)^{6}\right]. \quad (1)$$

Here, ε_0 is the vacuum permittivity, q_i and q_j are the charges of atoms i and j, ϵ_{ij} is the energy minimum of the LJ potential, and σ_{ij} is the LJ diameter. Water is described by the TIP4P/2005 model.[33] This water model has a LJ interaction site at the oxygen and charges q$_H$ and q$_M$ located, respectively, at the hydrogen positions and at a point M placed near the oxygen along the H–O–H bisector (see Table I). For monovalent ions (Na$^+$, K$^+$, Li$^+$, and Cl$^-$), the scaled value of the charge is $|q_{scaled}| = 0.85$ since that was the choice for the Madrid model proposed previously.[72] This choice was suggested by Kann and Skinner[57] and guarantees a good description of the infinite dilution properties of monovalent ions in TIP4P/2005 water since it compensates the low dielectric constant of the water model. For consistency, we assign a charge of 1.7 (in electron units) to monoatomic divalent cations (Mg^{2+} and Ca^{2+}). Since we use scaled charges, the notation Na$^+$ (or Mg^{2+}, etc.) does not reflect the ionic charge. However, for simplicity, we respect throughout this paper the common ionic notation.

Modeling sulfate (a highly symmetric polyatomic anion) as a rigid body pose some problems when one intends to carry out molecular dynamics using constraints to preserve the molecular geometry. To avoid the inconveniences, the sulfur atom cannot have mass and should be treated as a dummy atom. Of course, since the mass distribution does not affect the equilibrium thermodynamic properties within classical statistical mechanics, the sulfur mass can be distributed among the oxygen atoms. In this way, the total molecular mass is preserved, so most of the dynamical properties will not be affected. It may slightly affect the rotation dynamics of the sulfate group. In summary, we have modeled sulfate as a set of four interacting sites at the positions of the oxygen atoms in a tetrahedral arrangement and a masless site located on the sulfur atom. The experimental molecular weight is then distributed among the four oxygen atoms. In accordance to the choice for other ions, the net charge of the sulfate group is −1.7. There are several ways of distributing the net charge between the oxygen and sulfur atoms. We have found that a relatively wide range of values for the sulfur charge (q$_S$) may account of the properties of sulfate solutions

TABLE I. Parameters of the Madrid-2019 force field. Charges of the particles used in this work and geometric parameters of the water and sulfate molecules. Parameters for TIP4P/2005 water were taken from the work of Abascal and Vega.[33]

Particle charges (e)	
$q_{Na} = q_K = q_{Li} = 0.85$, $q_{Mg} = q_{Ca} = 1.70$, $q_{Cl} = -0.85$	
$q_S = 0.90$, $q_{O_s} = -0.65$, and $q_H = -q_M/2 = 0.5564$	

H$_2$O geometry	SO$_4$ geometry
Distance d$_{OH}$ = 0.9572 Å	Distance d$_{OS}$ = 0.149 Å
Distance d$_{OM}$ = 0.1546 Å	Distance d$_{OO}$ = 0.243 316 Å
Angle H–O–H = 104.52°	Tetrahedral structure

although the parameters of the LJ interactions are slightly dependent on the particular choice of q_S. We have finally assigned it a charge of 0.90 (in electron units). The geometry of the sulfate molecules and the charges of the sites used in this work are presented in Table I.

We proceed now to describe how the parameters of the LJ interactions have been obtained. The order in which the parameters of the force field were optimized was as follows:

- Parameters of Na^+ and Cl^-.
- Parameters of cations (using the parameters of Cl^- obtained in the previous step) from studies of the corresponding cation chlorides.
- Parameters of SO_4^{2-} from studies of Na_2SO_4.
- Fine tuning of the $K^+ - SO_4^{2-}$, $Li^+ - SO_4^{2-}$, and $Mg^{2+} - SO_4^{2-}$ cross interactions from studies of the corresponding sulfate solutions.

The following set of target properties has been used to determine the optimal LJ interaction parameters for each salt:

- Densities of the aqueous solution at moderate (around 1 m) and high concentrations (close to the solubility limit).
- Densities of the molten salt (at the experimental melting temperature) and of the solid at ambient conditions (only when the stable solid had the rock salt structure). For reasons that will be explained below, the target values for the densities of the molten salts and solids were not just the experimental ones.
- Position of the main peak of the ion-water radial distribution function and hydration numbers.
- A moderate degree of clustering of ions near the experimental value of the solubility limit. In practice, this is achieved by imposing a number of ionic pairs below 0.5 at the experimental value of the solubility. This indirectly guarantees that the solubility of the model is not too low when compared to experiments (see Ref. 82 for a detailed discussion of this). Note that experimental values of the number of CIP at the solubility limit are, in general, not available.

In Table II, the experimental melting temperatures[83] and solubility limits[84,85] for the salts considered in this work are presented. As it can be seen, the solubility of all the salts (with the exception of $CaSO_4$) is moderate or high.

Let us now expand a little bit our discussion on the target properties. The strongest forces in ionic systems come from electrostatic interactions, more, in particular, from the potential between unlike-charged particles which are somehow balanced by the repulsive forces at short distances. When ionic crystals are dissolved, the ions fall quite apart and the ionic interactions are much weaker and are replaced by the ion-water interactions. In both systems, the interactions between nonidentical particles (cation-anion, ion-water) are dominant. This is in contrast with typical choices of force fields for nonionic systems which usually define the parameters for the interactions between particles of the same type and evaluate the cross interactions using some (arbitrary) rules. Apart of the use of scaled charges, one of the main ideas behind this work is that the parameters associated with the cation-anion and ion-water interactions should be explicitly optimized. Since the charges of the particles are

TABLE II. Experimental melting temperature for anhydrous salt[83] and salt solubility in water at 25 °C reported in molality units.[84,85]

Salt	Melting temperature (K)	Solubility at 25 °C (m)
LiCl	883.15	19.95
NaCl	1073.85	6.15
KCl	1044.15	4.81
$MgCl_2$	987.15	5.81
$CaCl_2$	1048.15	7.3
Li_2SO_4	1132.15	3.12
Na_2SO_4	1157.15	1.96
K_2SO_4	1342.15	0.69
$MgSO_4$	1397.15	3.07
$CaSO_4$	1733.15	0.02

fixed, the optimization process mostly affects the σ_{ij} and ϵ_{ij} (with $i \neq j$) parameters of the Lennard-Jones potential. In this way, the density of the solution is paramount to determine the ion-water potential (note that, given the excellent performance of TIP4P/2005, the departures of the solution densities from that of pure water provides a direct measure of the ion-water interactions). We have thus optimized the LJ parameters of the ion-water interactions in order to reproduce the density of moderate to high concentrated solutions.

On the other hand, in order to optimize the anion-cation parameters, we have used information from the experimental densities of molten salts and solid phase. When developing the Madrid model for aqueous NaCl, we also considered the solid phase in the optimization process. However, here, we have changed the approach in a qualitative way. Now, we do not attempt to predict the exact experimental values of the densities neither of the melt nor of the solid since for most of the salts, we failed to reproduce simultaneously the densities of the melt and those of the solution at high concentrations. Thus, we recognize that models with scaled charges should not reproduce the experimental values of ionic systems without water (accurate predictions in this case could only be obtained when using the full ionic charges). We observed that, typically, the density of the melt/solid increases by about 20/8% when the charge of the ions changes from 0.85 to 1 while keeping the LJ parameters. Thus, our target value for the density of the melt/solid was around 20/8% smaller than the experimental value. Besides, this allows the possibility of developing in the future a polarizable version of the force field described here where the charge of the ions changes with the environment and returns to the full charge values in the melt and/or solid phase.

As commented above, cation-cation and/or anion-anion interactions have a minor impact in the final force field and we have usually accepted the values of previous works. In some cases (mostly for the interactions between ions of different types but carrying the same charge sign), we have used the Lorentz-Berthelot (LB) combining rules

$$\sigma_{ij} = \frac{\sigma_{ii} + \sigma_{jj}}{2}, \quad \epsilon_{ij} = \sqrt{\epsilon_{ii}\epsilon_{jj}}. \quad (2)$$

After these steeps, we had a preliminary set of parameters which allowed us to compute the radial distribution functions of the

TABLE III. Parameters of the Madrid-2019 force field. Lennard-Jones σ_{ij} parameters (in nm) for electrolyte solutions in TIP4P/2005 water containing Li$^+$, Na$^+$, K$^+$, Mg^{2+}, Ca^{2+}, Cl$^-$, and SO$_4^{2-}$. Some σ_{ii} of cations were taken from the literature (Li,[15] Na,[72] Mg,[27] Ca,[45] O$_w$,[33] and S[86]). In cases where a numerical value is not given, we suggest to follow Lorentz-Berthelot (LB) combination rules. LB(+) indicates that, in these cases, we have checked LB combining rules in binary or ternary solutions with satisfactory results. O$_w$ and O$_s$ denote the oxygen site in water and sulfate, respectively.

	Li	Na	K	Mg	Ca	Cl	O$_w$	S	O$_s$
Li	0.143 970	LB(+)	LB	LB	LB	0.270 000	0.212 000	LB(+)	0.284 485
Na		0.221 737	LB(+)	LB(+)	LB(+)	0.300 512	0.260 838	LB(+)	LB(+)
K			0.230 140	LB	LB	0.339 700	0.289 040	LB(+)	0.320 000
Mg				0.116 290	LB	0.300 000	0.181 000	LB(+)	0.240 645
Ca					0.266 560	0.315 000	0.240 000	LB	LB
Cl						0.469 906	0.423 867	LB(+)	LB(+)
O$_w$							0.315 890	LB(+)	0.340 445
S								0.355 000	LB
O$_s$									0.365 000

TABLE IV. Parameters of the Madrid-2019 force field. As in Table III, but for Lennard-Jones ϵ_{ij} parameters (in kJ/mol).

	Li	Na	K	Mg	Ca	Cl	O$_w$	S	O$_s$
Li	0.435 090	LB(+)	LB	LB	LB	1.282 944	0.700 650	LB(+)	0.803 609
Na		1.472 356	LB(+)	LB(+)	LB(+)	1.438 894	0.793 388	LB(+)	LB(+)
K			1.985 740	LB	LB	1.400 000	1.400 430	LB(+)	1.289 519
Mg				3.651 900	LB	3.000 000	12.000 00	LB(+)	2.748 743
Ca					0.507 200	1.000 000	7.250 000	LB	LB
Cl						0.076 923	0.061 983	LB(+)	LB(+)
O$_w$							0.774 908	LB(+)	0.629 000
S								1.046 700	LB
O$_s$									0.837 400

aqueous solutions and calculate the position of the ion-water first peak, the CIP at high concentrations, and the hydration numbers to check if the overall results were reasonable. These calculations provided a feedback, so the final refined parameters are the outcome of some trial and error methodology.

Our starting point was the recently proposed Madrid model, a force field for NaCl in water. However, it was clear from the beginning that the densities predicted for MgCl$_2$ and CaCl$_2$ were slightly lower than the experimental ones. Since, in those attempts, we tried to optimize the parameters for Mg^{2+} and Ca^{2+} while keeping the parameters of Cl$^-$ from the Madrid model that was suggesting that the contact distance between Cl$^-$ and water was too large, we thus reduced the parameter σ_{Cl-O_w} from the value in the Madrid model (0.426 867) to 0.423 867 nm. This is certainly a small change, but, to keep the excellent predictions of the Madrid model, it was necessary to slightly modify the rest of parameters. This new force field for aqueous NaCl is denoted as the Madrid-2019 model and can be regarded as a minor modification of the original Madrid model (a comparison of the parameters of both models is given in the supplementary material). In Sec. IV, we shall show that the performance of both models is essentially the same.

The parameters of the Madrid-2019 force field are presented in two separated tables. The values of σ for the LJ interactions are given in Table III, while the ϵ parameters are shown in Table IV

(some σ_{ii} and ϵ_{ii} parameters were taken from the literature: Li,[15] Na,[72] Mg,[27] Ca,[45] O$_w$,[33] and S[86]). The geometry and charges were presented previously in Table I. When for a certain interaction one reads LB, it means that the corresponding value was obtained from the application of the LB combining rule [Eq. (2)]. When a + symbol is written in addition to the word LB, then it means that the LB rule has been validated in this work by the results of at least one mixture.

III. SIMULATION DETAILS

NVT and NPT molecular dynamics (MD) simulations have been performed using the GROMACS package.[87] In all runs, the time step was 2 fs. The cut-off radii were fixed at 1 nm for both electrostatics and Lennard-Jones interactions. Long range corrections to the LJ part of the potential energy and pressure were included. Coulombic interactions were evaluated with the smooth PME method.[88] We have used the Nosé-Hoover thermostat[89,90] with a relaxation time of 2 ps to keep a constant temperature, except in the case of solid state simulations where the v-rescale algorithm[91] has been selected. NPT simulations were performed at 0.1 MPa (and in some cases at 200 MPa) with Parrinello-Rahman pressure coupling[92] with a relaxation time for the barostat of 2 ps. The LINCS

algorithm[93,94] has been used to constrain water geometry for most of the systems. In the case of salts containing the sulfate anion, we used SHAKE[95] for both water and sulfate because this algorithm is more efficient for the sulfate group.

To calculate equilibrium properties like density or radial distribution function for liquid systems, we have performed simulations of 50 ns for a system containing 555 water molecules. This choice is useful because 10 ions of any type correspond to a 1 m solution of that ion. The number of contact ion pairs (CIPs) can be computed from the cation-anion RDF as

$$n^{CIP} = 4\pi\rho_{\pm} \int_0^{r_{min}} g_{+-}(r) \, r^2 \, dr, \qquad (3)$$

where g_{+-} is the cation-anion RDF and $\rho_{\pm}$ is the number density of cation or anions. The integral upper limit r_{min} is the position of the first minimum in the RDF (if any) which must be located at a similar distance to that of the cation-O_w RDF. It is a good idea to plot simultaneously the cation-anion and cation-O_w RDFs to determine if one is really evaluating the CIP or a solvent separated ion pair. To check for the absence of precipitation, we typically performed a long run (of about 40 ns) for a system containing 555 × 8 = 4440 molecules of water and the corresponding number of ions to give the experimental value of the solubility limit and checked for aggregation.

The transport properties as viscosities and/or diffusion coefficient were also determined in a system having 4440 water molecules. The methodology used to compute the viscosity is similar to that described in previous works.[96] A previous NPT simulation is required to calculate accurately the volume of the system. After that, an NVT simulation was performed lasting between 50 ns and 200 ns. Throughout the run, the pressure tensor $P_{\alpha\beta}$ was calculated and saved on disk every 2 fs. Finally, the Green-Kubo formula was used

$$\eta = \frac{V}{kT} \int_0^\infty \langle P_{\alpha\beta}(t_0) \, P_{\alpha\beta}(t_0 + t) \rangle_{t_0} \, dt. \qquad (4)$$

The actual upper limit of the integral should be much higher than that of pure water. In fact, for some solutions, we have used values of the order of several hundreds of picoseconds (for pure water, the upper limit is usually of the order of 10 ps).

The self-diffusion coefficient has been evaluated using the Einstein relation

$$D = \lim_{t \to \infty} \frac{1}{6t} \left\langle [\vec{r}_i(t) - \vec{r}_i(0)]^2 \right\rangle, \qquad (5)$$

where $\vec{r}_i(t)$ and $\vec{r}_i(0)$ are the position of the i-th particle at time t and a certain origin of time t = 0 and the $\langle [r_i(t) - r_i(0)]^2 \rangle$ term is the mean square displacement (MSD).

The densities of the melt and of the solid (with the rock salt structure) were obtained for systems containing 1000 ions. Simulations typically lasted 10 ns. For the melts, the simulations were performed at 0.1 MPa and at the melting temperature of the anhydrous salt (see Table II). The simulations of the solid were performed at 298.15 K and 0.1 MPa for the salts exhibiting a NaCl solid structure: LiCl, NaCl, and KCl. All these solids were found to be mechanically stable after a 10 ns run.

IV. RESULTS

A. 1:1 electrolyte solutions

1. Sodium chloride

As mentioned above, we realized soon in this research that setting the parameters of the chloride anion as in the original Madrid model did not allow us to reproduce with high accuracy the densities of MgCl$_2$ and CaCl$_2$ solutions. This was possible when we decreased by 0.003 nm the value of σ_{Cl-O_w}. This slight change forced a fine tuning of the rest of parameters. The new Madrid-2019 model can be regarded as a minor modification of the original one (see the supplementary material which also includes a topol.top file of GROMACS with the parameters of the potential). Figure 1 shows the density predictions using different models for NaCl solutions. In the OPLS-TIP4P/2005[2] and JC-TIP4P/2005[72] models, the ionic parameters are those of the OPLS and Joung-Cheatham[15] force fields, respectively, and the water model is TIP4P/2005. Since all these force fields use the same model for water, the differences in performance are due to differences the ion-water and ion-ion interactions. As can be seen in the plot, the calculations for the Madrid-2019 force field are in better agreement with the experimental data[97–99] than those of OPLS-TIP4P/2005 and JC-TIP4P/2005. The results of this work are quite similar to those of the previous Madrid model although we notice a slight improvement in the 200 MPa isobar at high concentrations.

In Table V, densities for solid (at 0.1 MPa and 298.15 K) and molten salts (at 0.1 MPa and the experimental melting temperature) are presented. For each system, two results are shown. The first one corresponds to the density of the Madrid-2019 force field using the scaled charges q_{scaled}. The second one shows the density obtained with the same set of parameters as in the Madrid-2019 model but replacing the scaled charges by the standard values q (i.e., 1 for monovalent and 2 for divalent ions). The densities of the molten NaCl using the Madrid-2019 force field are 15% lower
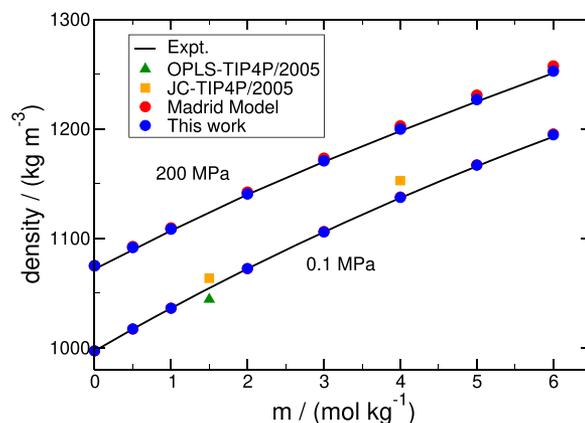
FIG. 1. Density as a function of molality for aqueous NaCl solutions at T = 298.15 K for the 0.1 MPa and 200 MPa isobars. Values from this work are shown with blue circles, the Madrid model predictions[72] are shown with red circles, and the results for the OPLS-TIP4P/2005[2] and JC-TIP4P/2005[72] force fields are represented by a green triangle and orange squares, respectively. The experimental data[97–99] are shown as continuous lines.

TABLE V. Densities of the molten salts (at 0.1 MPa and the experimental melting temperature[83]) and of the anhydrous salt crystals (at 0.1 MPa and 298.15 K). Values of this work are given under columns labeled q_{sc} and q which are obtained using scaled charges and total charges for the ions, respectively.

Salt	Melt density			Solid density		
	q_{sc}	q	Expt.	q_{sc}	q	Expt.
LiCl	1237	1443	1502	1907	2075	2068
NaCl	1331	1634	1556	2050	2218	2165
KCl	1236	1531	1527	1834	1984	1984
MgCl$_2$	1581	1779	1680			
CaCl$_2$	1754	2083	2085			

FIG. 2. Shear viscosity curves as a function of concentration for aqueous LiCl, NaCl, and KCl systems at 298.15 K and 0.1 MPa. Result from this work is shown with blue circles, those from the Madrid model[72] is shown with red circles, and NaCl JC-TIP4P/2005[55] is shown in orange squares. The continuous lines are our fit of experimental data taken from Refs. 101 and 102 and references therein. NaCl and LiCl values were shifted up one and three units, respectively, for better legibility.

than in the experiment. Concerning the density of the crystal, the result of our model is about 5% below the experimental one. These departures greatly decrease when the scaled charges are replaced by the full ones. This fact seems to indicate that the relative size of the ions is well captured by the parameters presented in Tables III and IV for the ion-ion interactions. In other words, the removal of water from the solution translates into a change of the effective ionic charges from those used in this work to the usual integer numbers in the crystal or the melt. In this way, the nontransferability of the force field between the solution and the pure salt in the condensed state is the price to pay for a better description of the solution properties. Note finally that the results of Table V indicate that the comments made here for NaCl maybe extended to other salts; the typical deviations between the scaled charged model and the full charged ones are less than 20% for the melts and less than 8% for the crystal.

For the sulfate molecules, we are not presenting results with the unscaled charges as there are many ways of distributing the charge between the oxygen and the sulfate to achieve a net charge of −2.

To gain further evidence of the quality of the Madrid-2019 force field, we have analyzed some structural results. We have computed the ion-ion and ion-water radial distribution functions at 6 m, a concentration close to the experimental value of the solubility limit. From the RDF, it is possible to evaluate the number of contact ion pairs [see Eq. (3)] and the hydration numbers (i.e., the number of water molecules around each ion). The latter is computed as in Eq. (3) but replacing $\rho_\pm$ by ρ_w and $g_{+-}(r)$ by $g_{ion-O_w}(r)$ instead. The results are summarized in Table VI and compared with experimental X-ray and neutron diffraction data collected from

the work of Marcus.[100] The number of CIP is an important property when studying electrolytes. A high value provides an indirect indication of cluster formation and/or precipitation of the salt. For 1:1 electrolytes with solubility lower than 10 m, Benavides et $al.$[82] suggested that the number of CIP must be below 0.5 to be sure that precipitation and/or aggregation of ions has not occurred. For NaCl, we have found a value of 0.17 at 6 m. In fact, aggregation was not found at this concentration in long runs of large systems. The hydration numbers for Na$^+$ and Cl$^-$ are 5.4 and 5.9 waters, respectively. These values are within the range reported in experiments.[100] The d_{Na-O_w} and d_{Cl-O_w} distances are 2.25 Å and 3.10 Å, respectively, to be compared to the experimental estimations 2.33 Å and 3.05 Å.

Two transport properties have been evaluated in this work: the shear viscosity and the self-diffusion coefficients. Figure 2 shows the shear viscosity for NaCl aqueous systems as a function of the concentration at 298.15 K and 0.1 MPa. The results of the Madrid-2019 force field are again quite similar to those of the Madrid force field. In general, the agreement with experimental data[101,102] is excellent at low concentrations. The dependence with concentration follows

TABLE VI. Structural properties for 1:1 electrolyte solutions at 298.15 K and 0.1 MPa. Number of contact ion pairs (CIPs), hydration number of cations (HN$_c$) and anions (HN$_a$), and position of the first maximum of the cation-water (d_{c-O_w}), and anion-water (d_{a-O_w}) RDFs. In parentheses are experimental data taken from the work of Marcus[100] and references therein. Properties were calculated for LiCl, NaCl, and KCl solutions at 12 m, 6 m, and 4.5 m concentrations, respectively.

Salt	CIP	HN$_c$	HN$_a$	d_{c-O_w} (Å)	d_{a-O_w} (Å)
LiCl	0.01	4(3.3—5.3)	5.9(4—7.3)	1.84(1.90—2.25)	3.03(3.08—3.34)
NaCl	0.17	5.4(4—8)	5.9(5.5—6)	2.33(2.41—2.50)	3.05(3.08—3.20)
KCl	0.38	6.5(6—8)	5.8(6—8)	2.73(2.60—2.80)	3.03(3.08—3.16)

TABLE VII. Self-diffusion coefficients of cations and anions (D_c, D_a) as a function of concentration (in 10^{-5} cm^2/s units) for electrolyte water solutions at 298.15 K and 0.1 MPa. A comparison is done with experimental results at infinite dilution.[103] Water diffusion in electrolyte solutions relative to water diffusion in pure water, D_w^{salt}/D_w^{pure}, is also shown. Experimental data at 1 m were taken from Müller and Hertz,[104] where $D_w^{pure} = 2.3$, and in our simulation $D_{TIP4P/2005}^{pure} = 2.14$ without applying the finite-size correction of Yeh and Hummer.[105]

Salt	D_c			D_a			D_w^{salt}/D_w^{pure}	
	Sim		Expt.	Sim		Expt.	Sim	Expt.
	1 m	0.5 m	0 m	1 m	0.5 m	0 m	1 m	1 m
LiCl	0.81	0.92	1.03	1.31	1.38	2.03	0.84	0.91
NaCl	0.99	1.22	1.33	1.33	1.39	2.03	0.89	0.94
KCl	1.63	1.70	1.96	1.52	1.45	2.03	0.97	1.03
MgCl$_2$	0.41	0.64	0.705	0.89	1.30	2.03	0.67	0.73
CaCl$_2$	0.55	0.63	0.791	1.10	1.23	2.03	0.74	0.82
Li$_2$SO$_4$	0.63	0.82	1.03	0.68	0.72	1.07	0.74	
Na$_2$SO$_4$	0.82	0.85	1.33	0.76	0.91	1.07	0.79	
K$_2$SO$_4$	. . .	1.60	1.96	. . .	0.86	1.07	. . .	
MgSO$_4$	0.40	0.59	0.705	0.58	0.78	1.07	0.72	

the same trend as the experimental one, but the slope is somewhat overestimated, especially at very high concentrations. Anyway, our model improves considerably the results for JC-TIP4P/2005. This confirms that the scaling of the charges leads to a better description of the viscosity of NaCl(aq).

Numerical results for the self-diffusion coefficients of ions and water are presented in Table VII. The cation and anion self-diffusion coefficients were evaluated at two different concentrations (0.5 m and 1 m) to provide an idea of the value at low concentrations so that they can be compared to the experimental ones at infinite dilution.[103] The diffusivity of Na$^+$ seems to be in accordance with the experimental measurements, but that of Cl$^-$ differs to a certain extent from the experiment.[103] Finally, the performance of the force field for the ratio D_w^{salt}/D_w^{pure} is quite good in comparison with experimental data from Müller and Hertz.[104] For this ratio, we have not applied the finite-size correction to the water diffusion proposed by Yeh and Hummer.[105]

In summary, the main conclusion of the calculations for NaCl solutions is that the Madrid-2019 model yields quite similar results to those obtained with the original Madrid model for equilibrium, structural, and transport properties. We thus believe that other properties nonevaluated in this work will follow a similar pattern (for a more comprehensive discussion of the performance of the Madrid model, we refer the reader to our previous work[72]).

Figure 3 shows the behavior of the relative change of the dielectric constant, $\Delta\varepsilon_r = (\varepsilon_{solution} - \varepsilon_{H_2O})/\varepsilon_{H_2O}$, of the NaCl solutions at room temperature. Experimental results were taken from Refs. 106 and 107. As it can be seen, the relative decrease in the dielectric constant with the salt concentration is captured quite well by the Madrid-2019 force field even though the absolute values of the dielectric constant are not well described by the force field. The reason for this is that the TIP4P/2005 model of water does not reproduce well the experimental value of the dielectric constant of
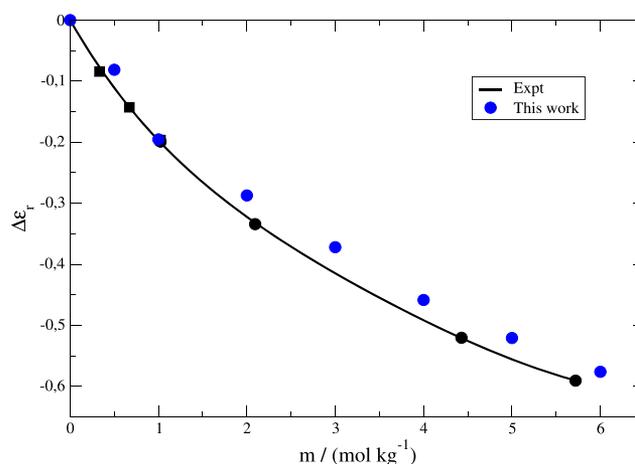
FIG. 3. Relative change of the dielectric constant as a function of the salt molality for NaCl aqueous solutions at 1 bar and 298.15 K. Results using the Madrid-2019 force field are shown in blue circles, and experimental values are also shown with a fitted curve of the data (black squares[106] and black circles[107]).

water (although the reason for this and possible ways to fix it have been discussed in detail in previous work[69,70]).

2. Potassium chloride

The densities of potassium chloride solutions are shown in Fig. 4. The agreement with experimental data is excellent along the whole concentration range. The relative failure of the MP-S/E3B model which also uses scaled charges[57] is probably due to the fact that the model underestimates the water density. For a concentration of 4.5 m, the K-O$_w$ RDF shows a first peak at 2.73 Å and the hydration number of K is 6.5 water molecules. At this concentration,
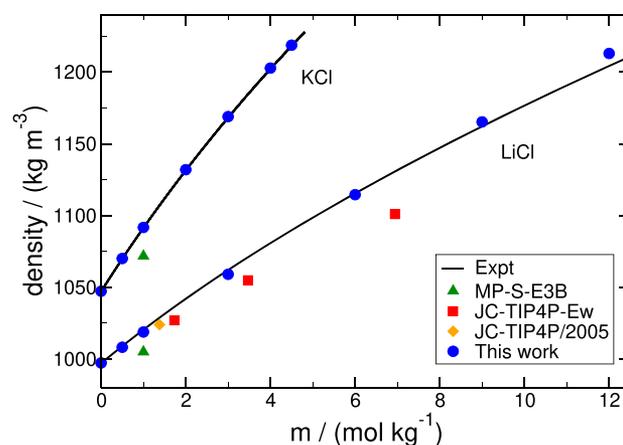
FIG. 4. Density as a function of molality at T = 298.15 K and 0.1 MPa for two 1:1 electrolyte aqueous solutions, LiCl and KCl. The symbols are as follows. Blue circles: this work, red squares: JC-TIP4P-Ew,[15] orange diamonds: JC-TIP4P/2005,[108] and green triangles: MP-S/E3B.[57] The continuous lines are our fit of experimental data taken from Refs. 101 and 109 and references therein. KCl values were shifted up 50 units for better legibility.
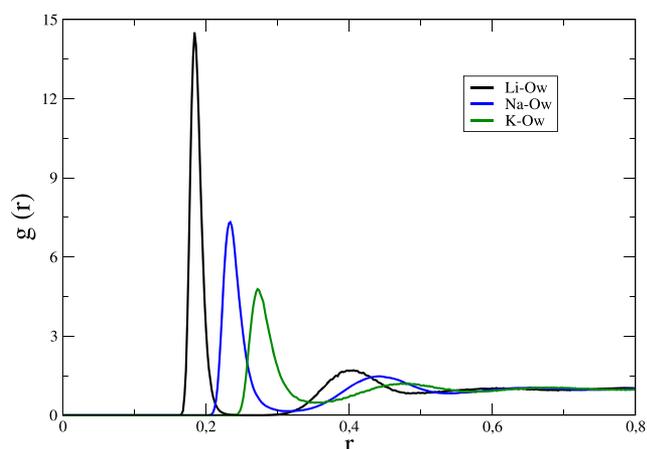
FIG. 5. Cation-water oxygen radial distribution function for 1:1 electrolyte solutions at 298.15 K, 1 bar, and 1 m as were obtained with the Madrid-2019 model in solutions: LiCl (black line), NaCl (blue line), and KCl (green line).

FIG. 6. Density curves for $MgCl_2$ and $CaCl_2$ in water solutions at 298.15 K and 0.1 MPa. Blue circles are the data from this work, green triangles are the MFN-SPC/E results,[23] and red square represents the calculations for the OPLS-TIP4P/2005 model. The continuous lines are our fit of experimental data taken from Refs. 102 and 109 and references therein. For a better appraisal, the $CaCl_2$ densities have been shifted up 100 units.

the maximum in the Cl-O_w RDF is located at 3.03 Å and the corresponding coordination number is 5.8 water molecules, very similar to that in LiCl and NaCl solutions. As for NaCl, the structural results are in accordance with the experimental estimations. At the highest simulated concentration, the CIP takes an acceptable value of 0.38 without cluster formations during the whole simulation. In contrast, precipitation of KCl has been reported in previous work when using models with full ionic charges.[44]

The viscosities of KCl solutions were already shown in Fig. 2 together with the results for other 1:1 electrolytes. The comparison with the experiment is quite remarkable, especially, because the model correctly predicts the small dependence of η on concentration. The diffusion coefficients of the cation at 1 m and 0.5 m (see Table VII) seem to point toward the experimental value at infinite dilution. As to the Cl$^-$ anion, despite that there is some improvement in the self-diffusion respect to LiCl and NaCl cases, the results of the model are clearly lower than those from the experiment. On the other hand, the presence of KCl does not affect much the diffusion coefficient of water (the relative water diffusion at 1 m is 0.97). In experiments, the same is true although the salt changes the diffusion coefficient in the opposite direction as it increases to 1.03 (this tendency is correctly described by the MP-S/E3B model[57]).

3. Lithium chloride

Figure 4 shows the equation of state for LiCl in water 298.15 K and 0.1 MPa compared to the experiment and to the results of

other force fields. The performance of the Madrid-2019 is better than that of the MP-S/E3B model which also uses scaled charges. Results for force fields that do not use the concept of charge scaling are also presented, in particular, for JC/TIP4P-Ew[15] and its modified version[108] which replaces the TIP4P-Ew water model by TIP4P/2005. The predictions of the Madrid-2019 force field are in excellent agreement with experimental data.[109] Although slight deviations maybe noticed at very high concentrations, the departure from the experiment at 12 m is less than 1%. In contrast, the results of the rest of force fields are not accurate enough at low concentrations and, in the case of JC/TIP4P-Ew, it predicts a much less steeper slope.

Some structural results for a 12 m concentration were presented in Table VI. The CIP are very low at this concentration. This is probably due to a strong hydration layer which prevents close cation-anion contacts. The Li$^+$ ions are hydrated with four water molecules which are consistent with the experimental values.[100] In line with other monovalent halides, the hydration number of Cl$^-$ is 5.9. The ion-water distances at the first maximum of the RDF seem a bit underestimated, about 3% below the experimental estimations. More consistent results were found for other models; see Table VIII in the work of Kann and Skinner.[57]

The Madrid-2019 model exaggerates the dependence of the viscosity with concentration (see Fig. 2). This is a common trend for all

TABLE VIII. As in Table VI but for 2:1 electrolyte solutions. Properties in solution were calculated at 5 m and 6 m for $MgCl_2$ and $CaCl_2$, respectively. CIP is just the number of anions in contact with the cation.

Salt	CIP	HN$_c$	HN$_a$	d$_{c-O_w}$ (Å)	d$_{a-O_w}$ (Å)
MgCl$_2$	0	6(6—8.1)	5.9(6)	1.92(2.00—2.11)	3.03(3.13—3.16)
CaCl$_2$	0.02	7.1(5.5—8.2)	6.2(5.8—8.2)	2.38(2.39—2.46)	3.03(3.12—3.25)
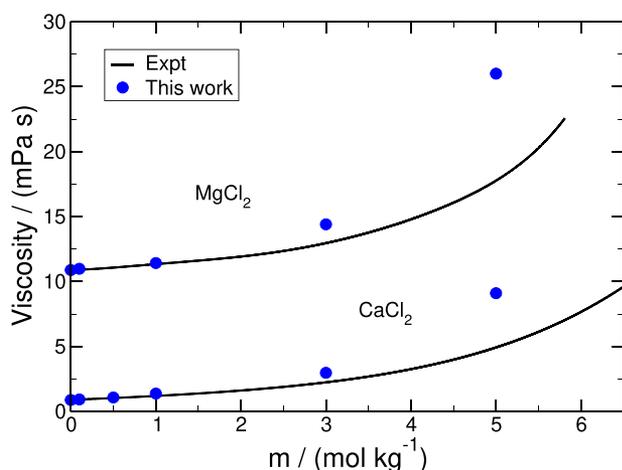
FIG. 7. Shear viscosity as a function of molality for aqueous $MgCl_2$ and $CaCl_2$ solution at 298.15 K and 0.1 MPa. Result from this work is shown with blue circles, and the continuous lines are our fit of experimental data taken from Refs. 101 and 102 and references therein. $MgCl_2$ values were shifted up ten units.

FIG. 8. Cation-water oxygen radial distribution function for 2:1 electrolyte solutions at 298.15 K, 1 bar, and molality 1 as were obtained with the Madrid-2019 model in $MgCl_2$ solutions (black line) and $CaCl_2$ solutions (blue line).

1:1 electrolytes although it seems that the deviation between simulation and experiment becomes larger as the size of the cation becomes smaller. It is to be noticed that the differences between the simulation and experiment are much larger for models with full ionic charges. Thus, the charge scaling alleviates but does not correct completely the dependence of the viscosity on salt concentration. Concerning the values of the diffusion coefficient of Li at infinite dilution, the results obtained in this work seem reasonable as compared to the experimental value at infinite dilution. Note that the differences between the diffusion of the chloride anion in NaCl, KCl, and LiCl solutions are quite modest suggesting that the effect of the counter ion is small at low concentrations. The predictions for the water diffusion agree reasonably with the experimental data, and the discrepancy is about 8% (see Table VII).

Finally, we shall present the cation-oxygen radial distribution functions for LiCl, NaCl, and KCl. They are presented in Fig. 5. As it can be seen, the obtained values reflect the size of the cations and the stronger hydration of the small cations.

B. 2:1 electrolyte solutions

1. Magnesium chloride

Figure 6 presents the densities of $MgCl_2$ solutions at 298.15 K and 0.1 MPa. The agreement with the experimental data[102,109] is quite good. At high concentrations, the deviations are of about 1%. The results obtained with the OPLS force field in combination with TIP4P/2005 are also shown for a concentration of 3 m. The deviation from the experiment is quite noticeable for this model that uses full ionic charges.

Structural properties at 5 m are summarized in Table VIII. The hydration sphere around Mg^{2+} contains exactly six water molecules. No anions are able to enter within the hydration shell of the cations (hence, the CIP is 0) meaning that the interaction between Mg^{2+} and
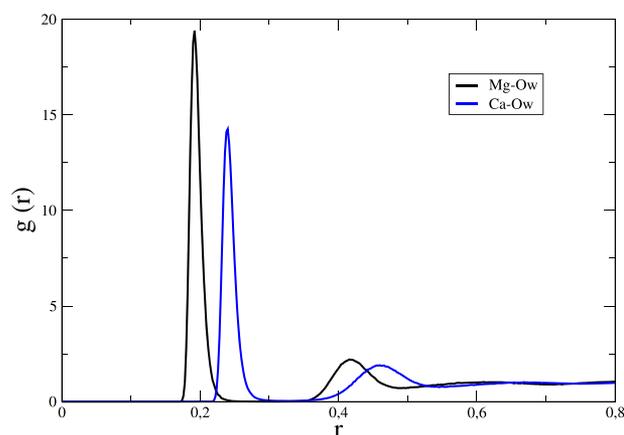
water is very strong. This is a well known result. Not surprisingly $MgCl_2$ often precipitates as hexahydrate. The second hydration shell is found at 4.18 Å with a coordination number of 13 waters in agreement with values reported in the literature (see Table III in the work of Zhang *et al.*[110]). The hydration number for Cl^- is 5.9 in agreement with the experiment. For both the cation and anion, the position of the first peak of the ion-O_w RDF lies at a shortest distance than the experimental estimations. This deserves a comment. It is somewhat surprising that, even though the model is able to reproduce extraordinary well the density of both pure water and the solution, the distance of the ions to the oxygen atoms in the first hydration shell is smaller than that reported from scattering experiments. It should be pointed out that extracting individual RDF from scattering
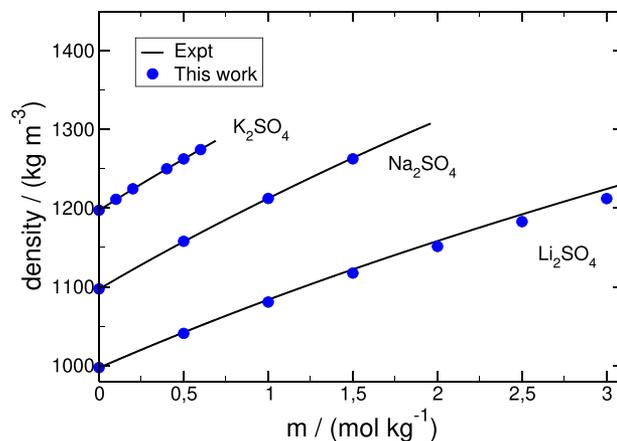
FIG. 9. Density as a function of salt concentration for Li_2SO_4, Na_2SO_4, and K_2SO_4 aqueous solutions at T = 298.15 K and 0.1 MPa. Blue circles are the results from this work, and the continuous lines are our fit of experimental data taken from Refs. 102, 109, and 111 and references therein. Data for Na_2SO_4 and K_2SO_4 are shifted up 100 and 200 units, respectively.

TABLE IX. As in Table VI but for 1:2 electrolyte solutions. Properties in solution were calculated for Li_2SO_4, Na_2SO_4, and K_2SO_4 at 3 m, 1.5 m, and 0.6 m, respectively. CIP is just the number of cations in contact with the sulfate group.

Salt	CIP	HN_c	HN_a	d_{c-O_w} (Å)	d_{S-O_w} (Å)	$d_{O_s-O_w}$ (Å)
Li_2SO_4	0	4(3.3—5.3)	13(6.4—8.1)	1.84(1.90—2.25)	3.75(3.67—3.89)	3.00(2.84—2.95)
Na_2SO_4	0.37	5.5(6)	13(6.4—8.1)	2.33(2.41—2.50)	3.75(3.67—3.89)	3.02(2.84—2.95)
K_2SO_4	0.88	6.5(6—8)	12(6.4—8.1)	2.73(2.60—2.80)	3.75(3.67—3.89)	3.02(2.84—2.95)

data is not a trivial task (especially in electrolyte solutions where one has contributions from many species). Even for pure water, experimental results for the RDF are improved year after year. For this reason, at this point, we believe that these experimental data should be regarded with care. This problem might be revisited in the future. In fact, it would be of interest to compute the structure factor from the simulations of this work and to see if they are able to describe the experimental data.

Figure 7 displays the concentration dependence of the viscosity of $MgCl_2$ solutions. The Madrid-2019 model is able to describe the experimental behavior up to 3 m concentration, but beyond this concentration, the deviation from the experiment is significant. Since viscosities can be measured with great accuracy, all the evidence presented so far points out that although the scaling of the charge provides a reasonable description of transport properties up to moderately high concentrations, the model fails at very high salt (although much less than models that use full ionic charges). Something is going on at high concentrations that are not captured by the force field of this work (and probably for the rest of the force fields proposed so far). This is a point that requires further work.

As to the diffusion of Mg^{2+} (see Table VII), our results at 1 m and 0.5 m concentrations extrapolate nicely to the experimental data

at infinite dilution. The model also captures quite well the sizable decrease in the diffusion coefficient of water when adding $MgCl_2$. Experimentally, the diffusion coefficient of water in a 1 m solution decreases to 73% to be compared to the prediction of the Madrid-2019 force field which yields 67%.

2. Calcium chloride

The densities of calcium chloride solutions are displayed in Fig. 6. The performance of the Madrid-2019 model is excellent up to 4 m. The deviations from the experiment increase slightly with the salt concentration, but they never exceed 1%. Also included in the plot are the data reported by Mamatkulov *et al.*[23] here denoted as MFN-SPC/E. The discrepancies from the experiment are now important and exceed 5% at high salt. The hydration number of Ca^{2+} is 7.1 water molecules (see Table VIII). The increase respect to that of Mg^{2+} is brought about by the increase in the cation size. In fact, the maximum of the Ca-O_w RDF appears at a higher distance, 2.38 Å, than in the lighter divalent cation. This distance is just at the lower limit of the range reported for experiments. The simulations of calcium chloride solution confirm that the hydration of the chloride anion is essentially insensitive to the counterion. Only the coordination number, 6.2, is marginally different.

The predictions for the viscosity of aqueous $CaCl_2$ follow a similar trend to those for $MgCl_2$. The model does a good job up to

FIG. 10. Shear viscosity as a function of concentration for aqueous Li_2SO_4, Na_2SO_4, and K_2SO_4 systems at 298.15 K and 0.1 MPa. Results of this work are shown as blue circles, and the continuous lines are our fit of experimental data taken from Refs. 101 and 102 and references therein. Values for Na_2SO_4 and Li_2SO_4 solutions were shifted up one and two units, respectively.
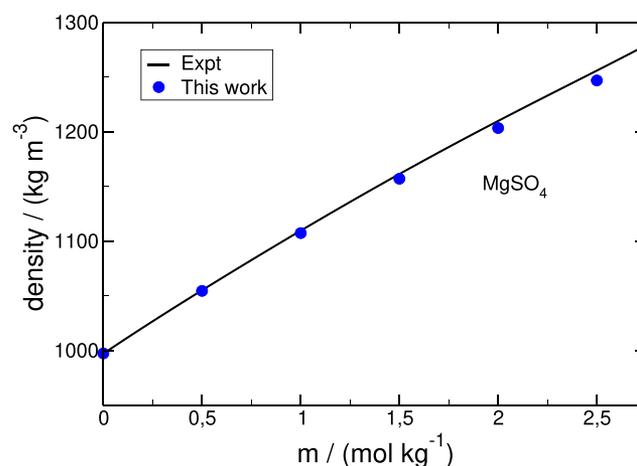
FIG. 11. Density as a function of molality for $MgSO_4$ solutions at 298.15 K and 0.1 MPa. In blue circles are data from this force field. The continuous line is our fit of experimental data taken from Refs. 102, 109, and 111 and references therein.

TABLE X. As in Table VI but for a 2.5 m MgSO$_4$ solution.

Salt	CIP	HN$_c$	HN$_a$	d$_{c-O_w}$ (Å)	d$_{S-O_w}$ (Å)	d$_{O_s-O_w}$ (Å)
MgSO$_4$	0	6(6)	13.5(6.4—8.1)	1.92(2.00—2.11)	3.75(3.67—3.89)	3.00(2.84—2.95)

3 m and fails beyond this salt concentration (although the deviations from the experiment are now somewhat smaller). The diffusion coefficients of Ca^{2+} in water seem to approach the experimental value at infinite dilution (see Table VII). The model also accounts quite acceptably for the experimental drop of the diffusivity of the water molecules in a 1 m solution (18% vs 26%). It is worth noting that the force field proposed in this work captures correctly the fact that, at 1 m concentration, the diffusion of water in 1:1 electrolytes decreases by about 5%, whereas the change is about 20% for 2:1 electrolyte solutions.

Finally, we shall present the cation-oxygen radial distribution functions for MgCl$_2$ and CaCl$_2$ solutions. Results are presented in Fig. 8. As it can be seen, the obtained values reflect the size of the cations and the stronger hydration of Mg^{2+} with respect to Ca^{2+}.

C. 1:2 electrolyte solutions: Lithium, sodium, and potassium sulfates

Before commenting the results for these systems, it is interesting to point out that the properties of sodium sulfate were used to optimize the sulfate parameters (fixing the Na parameters as obtained from NaCl systems). These parameters were mostly fixed for the rest of sulfates. In fact, we only modified slightly the LJ parameters of the cation-O$_s$ interaction and accepted the LB rule for other cross interactions.

Figure 9 shows the densities of the sulfates of monovalent cations as predicted by the Madrid-2019 force field. They are in excellent agreement with the experiment[102,109,111] although small deviations are visible at high concentrations in the case of Li$_2$SO$_4$.

Table IX collects the structural results obtained for 1:2 electrolytes with the sulfate as the anion. As also observed in 1:1 electrolytes, the hydration of the cation in sulfate solutions is strongly dependent of the cation size. No contact ion pairs are found for the smallest cation which explains the hygroscopic properties of lithium sulfate. The CIP of sodium sulfate is already significant, 0.37, and that of the potassium sulfate reaches a considerable value, 0.88. We did observe neither aggregation nor precipitation at the highest concentration of these salts, even after long runs. The hydration numbers and the location of the cation-O$_w$ peaks are almost exactly the same as those found previously in chloride solutions.

The solvation shell of SO$_4^{2-}$ is formed by about 13 water molecules, irrespective of the accompanying cation. Similar values have been reported in previous MD simulations.[86,112,113] In contrast, the experimental value is much lower, about 7. Given the enormous size of the sulfate anion, it is difficult to believe that it is hydrated by just 7 molecules of water.[113] The positions of the first maximum of the S–O$_w$ and the O$_s$–O$_w$ RDFs (which once again are independent of the corresponding counterion) are in reasonable agreement with the experimental values.

A look at Table VII indicates that the extrapolation of our simulated results for the diffusion coefficient of Li$^+$, Na$^+$, K$^+$, Mg^{2+}, and SO$_4^{2-}$ in sulfate solutions is in overall reasonable agreement with the reported experimental data at infinite dilution (although, very likely, the value for Li$^+$ is a bit low). We are not aware of experimental data on the diffusion coefficient of water in sulfate solutions. Our results show that, in accordance with the behavior in other electrolyte solutions, the presence of salt significantly reduces the diffusion of the water molecules.

The dependence of the viscosity of sulfate solutions on the salt concentration is shown in Fig. 10. The agreement between the results of the Madrid-2019 force field and the experimental ones is quite good for K$_2$SO$_4$ and Na$_2$SO$_4$. Certainly, given the relatively low solubility of these salts, the comparison is made for concentrations where the presence of ions does not affect dramatically the viscosity. Our model gives only a fair description of the viscosity of Li$_2$SO$_4$ solutions. Even at 1.5 m concentration, the departure from the experiment is much more significant that for Na$_2$SO$_4$. Since the slope of the simulation data is largely underestimated, the result at the solubility limit is almost one half the experimental value.

D. 2:2 electrolyte solutions: Magnesium sulfate

The equation of state of magnesium sulfate solutions is plotted and compared to experimental results in Fig. 11. The agreement
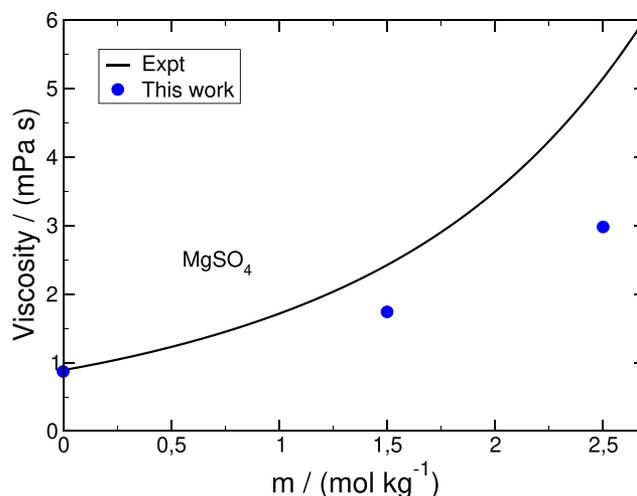
FIG. 12. Shear viscosity as a function of molality for MgSO$_4$ solutions at 298.15 K and 0.1 MPa. Blue circles are the data from this work, and our fit of experimental data taken from Refs. 101 and 102 (and references therein) is represented as a continuous line.

TABLE XI. Densities for ternary solutions at 298.15 K and 0.1 MPa rounded to entire units in kg/m^3. Experimental data from Refs. [114]–[118]. m_1 and m_2 are the molalities of the salts labeled (1) and (2), respectively. $m_{tot} = m_1 + m_2$ is the total concentration.

Expt.			This work			Expt.			This work		
m_{tot}	m_1/m_2	Density	m_{tot}	m_1/m_2	Density	m_{tot}	m_1/m_2	Density	m_{tot}	m_1/m_2	Density
NaCl (1) + LiCl (2) + H$_2$O						NaCl (1) + KCl (2) + H$_2$O					
2.106	0.4835	1057	2.1	0.50	1053	0.7935	0.3325	1032	0.8	1/3	1032
2.041	0.7253	1058	2.1	0.75	1056	2.3760	2.9867	1088	2.4	3	1089
1.976	1.0880	1059	1.9	10/9	1054	3.9943	0.3325	1148	4	1/3	1149
1.846	2.9013	1062	1.9	2.80	1060	4.6241	1.0010	1164	4.6	1	1164
NaCl (1) + MgCl$_2$ (2) + H$_2$O						NaCl (1) + CaCl$_2$ (2) + H$_2$O					
1.0992	9.9811	1044	1.1	10	1043	0.4060	0.3334	1028	0.4	1/3	1028
3.5006	5.9942	1138	3.5	6	1136	2.0102	3.0218	1094	2	3	1094
3.5099	0.1660	1210	3.5	1/6	1207	2.8055	1.0001	1158	2.8	1	1158
4.0106	0.3327	1224	4	1/3	1221	4.0519	3.0218	1178	4	3	1176
NaCl (1) + Na$_2$SO$_4$ (2) + H$_2$O											
0.5997	0.2001	1062	0.6	0.2	1062						
1.5000	1.9991	1092	1.5	2	1092						
1.9958	1.0026	1143	2	1	1142						
3.4999	5.9983	1155	3.5	6	1154						

is very good. Only at high salt, the simulations results underestimate the experimental density (about 1% at 2.5 m).

Structural properties for a 2.5 m solution are presented in Table X. Again, the magnesium is surrounded by 6 molecules of water located at a distance of 1.92 Å, and the sulfate anions are surrounded by 13.5 molecules of water at 3.75 Å. Also, the strong hydration layer disables the formation of contact ion pairs. At this concentration, no cluster aggregation is observed in simulations of large systems for long times.

In Fig. 12, the viscosity for magnesium sulfate in water is shown. The simulation results are well below the experimental ones, and the departures increase with concentration, a feature that was also found in MgCl$_2$. As with other salts containing a divalent ion, the diffusion coefficient of water in a 1 m solution decreases significantly respect to that of pure water (see Table VII).

Given the low solubility of CaSO$_4$ (i.e., 0.02 m), the densities for this salt are practically those of pure water and we shall not present results for this salt.

E. Ternary mixtures

In order to test and validate the force field of this work, we here present results for ternary mixtures of electrolytes (i.e., two salts and water). We use LB rules for those interactions that were not determined in the optimization process (see Tables III and IV). The calculations were done for a sample made of 555 water molecules and adjusting the number of salt molecules to the corresponding experimental concentration. Results for the Madrid-2019 force field are presented in Table XI together with experimental data.[114–118] The performance of the model is excellent. Some small deviations are in part due to the slight difference in concentration from the

simulations as compared to the experimental ones. Of course, the difference in concentration could be alleviated by using a larger system in the simulation. However, since our primary goal is to validate the proposed force field in systems not used in the optimization process, this test is already sufficient. The main advantage of presenting a force field is that it can deal with system of arbitrary compositions, pressures, and temperatures.

V. CONCLUSIONS

In this work, a new force field (denoted as Madrid-2019) for several ions in water has been proposed. The main conclusions are as follows:

- It is possible to design a force field that, using the concept of charge scaling and a factor of 0.85, is able to describe with high accuracy the densities of a number of salt solutions.
- Viscosities are also described quite well for concentrations up to 3 m. At higher concentrations, deviations are clearly visible, especially for systems containing a high charge density (Li$^+$, divalent ions).
- The description of the behavior of the diffusion coefficient also improves when compared to systems using full ionic charges.
- Complemented with the Lorentz-Berthelot rule, the force field is able to yield quite good predictions for ternary mixtures of electrolytes not used in the optimization of potential parameters.
- No precipitation or aggregation was found in the simulations performed at concentrations close to the experimental solubility limit. Thus, the absence of artifacts in the simulations is guaranteed at least up to this concentration.

- The improvement of the performance in aqueous solutions has a cost: the densities predicted for the crystal salts are typically 8% lower than the experimental ones. For molten salts, the deviations are even larger of the order of 20%.

Since the use of scaled charges for ions is a relatively recent idea, it is interesting to present some digressions on the possible limitations/possibilities of this approach.

The properties of the solid phase and/or the molten salts are defined by the ion-ion parameters. In contrast, the electrolyte properties at lower/moderate salt concentrations are mostly defined by ion-water parameters. Cation-anion parameters have little contribution until one reaches high concentrations. So interference between ion-water and cation-anion parameters should be observed only at high concentrations. Ideally, one would like to use integer charges for the interaction between the ions when in the melt phase and the solid phase and to restrict the use of scaled charges for the ions at low and moderate concentrations where the ions are solvated completely and the main contribution to the properties comes from the ion-water interactions. This is certainly possible when using polarizable force fields. However, this is not possible when using nonpolarizable models. At this point, one should conclude that the use of the scaled charges will benefit significantly the description of solutions at low and medium concentrations, moderately at high concentrations but not in the melt and/or solid phase.

Note also that scaled charges are used only to describe the potential energy surface. It is possible, in principle, to use different charges to describe the dipole moment surface both for the water molecule and for the ions. This was discussed in detail in Ref. 69 and also anticipated in the work by Leontyev and Stuchebrukhov.[62] It would, in principle, be possible to use scaled charges to describe the PES and integer charges to describe the DMS. This possibility will affect the way properties that measure the response of the system to an electric field (i.e., dielectric constant and electric conductivity) are calculated (although we have not implemented this possibility yet when presenting the results of the dielectric constant in Fig. 3). Indeed, if, for example, ion Cl^- passed from the anode to cathode, then the value of the transferred charge (contributing to the flux and conductivity expression) should be obviously just -1 and not -0.85. All these aspects should be analyzed in more detail in future work.

A price to pay for the use of scaled charges is that the solvation properties (i.e., hydration free energies) are too low. Thus, the chemical potentials of the salts in solution are smaller in absolute values when compared to the experiment as it was discussed in our previous work for NaCl.[82] However, it would possible to correct the calculated values by adding a theoretical expression denoted as the electronic contribution, as described in detail in Ref. 62 (see Eq. 2.10 in this reference). This would bring the simulations results in closer agreement with the experiment. This is the analogue of the self polarization energy correction proposed when the SPC/E model was introduced.[30] The water model itself did not reproduce the vaporization enthalpy, but it did so when the self polarization energy theoretical correction was included.

Overall, the first impression is that the use of scaled charges improves the description of ionic solutions when compared to current force fields that use full ionic charges.[45,57,82,119,120] It would also be of interest to determine solubilities and activity coefficients of the current force field. The overall performance of the force field for these properties remains to be seen. Further work is needed to fully explore the limits of this type of force fields. Although we used here the scaling factor 0.85 (which yielded good results for NaCl solutions), it would be interesting to check if other choices (i.e., 0.70, 0.75, 0.80, and 0.90) could led to force fields with an overall better performance.

SUPPLEMENTARY MATERIAL

See supplementary material for numerical values of densities and viscosities obtained in this work for several salt solutions, for a comparison of the Lennard-Jones parameters of the force field of NaCl of this work (Madrid-2019 model) to that proposed previously (Madrid model), and for a topol.top file of GROMACS including the Madrid-2019 force field.

ACKNOWLEDGMENTS

REFERENCES

[1] W. R. Smith, I. Nezbeda, J. Kolafa, and F. Moučka, Fluid Phase Equilib. **466**, 19 (2018).

[2] J. Chandrasekhar, D. C. Spellmeyer, and W. L. Jorgensen, J. Am. Chem. Soc. **106**, 903 (1984).

[3] T. Straatsma and H. Berendsen, J. Chem. Phys. **89**, 5876 (1988).

[4] J. Aqvist, J. Phys. Chem. **94**, 8021 (1990).

[5] L. X. Dang, J. Chem. Phys. **96**, 6970 (1992).

[6] D. Beglov and B. Roux, J. Chem. Phys. **100**, 9050 (1994).

[7] D. E. Smith and L. X. Dang, J. Chem. Phys. **100**, 3757 (1994).

[8] B. Roux, Biophys. J. **71**, 3177 (1996).

[9] Z. Peng, C. S. Ewig, M.-J. Hwang, M. Waldman, and A. T. Hagler, J. Phys. Chem. A **101**, 7243 (1997).

[10] S. Weerasinghe and P. E. Smith, J. Chem. Phys. **119**, 11342 (2003).

[11] K. P. Jensen and W. L. Jorgensen, J. Chem. Theory Comput. **2**, 1499 (2006).

[12] G. Lamoureux and B. Roux, J. Phys. Chem. B **110**, 3308 (2006).

[13] J. Alejandre and J.-P. Hansen, Phys. Rev. E **76**, 061505 (2007).

[14] P. J. Lenart, A. Jusufi, and A. Z. Panagiotopoulos, J. Chem. Phys. **126**, 044509 (2007).

[15] I. S. Joung and T. E. Cheatham III, J. Phys. Chem. B **112**, 9020 (2008).

[16] D. Corradini, M. Rovere, and P. Gallo, J. Chem. Phys. **132**, 134508 (2010).

[17] K. M. Callahan, N. N. Casillas-Ituarte, M. Roeselová, H. C. Allen, and D. J. Tobias, J. Phys. Chem. A **114**, 5141 (2010).

[18] H. Yu, T. W. Whitfield, E. Harder, G. Lamoureux, I. Vorobyov, V. M. Anisimov, A. D. MacKerell, Jr., and B. Roux, J. Chem. Theory Comput. **6**, 774 (2010).

[19] M. M. Reif and P. H. Hünenberger, J. Chem. Phys. **134**, 144104 (2011).

[20] M. B. Gee, N. R. Cox, Y. Jiao, N. Bentenitis, S. Weerasinghe, and P. E. Smith, J. Chem. Theory Comput. **7**, 1369 (2011).

[21] S. Deublein, J. Vrabec, and H. Hasse, J. Chem. Phys. **136**, 084501 (2012).

[22] A. H. Mao and R. V. Pappu, J. Chem. Phys. **137**, 064104 (2012).

[23] S. Mamatkulov, M. Fyta, and R. R. Netz, J. Chem. Phys. **138**, 024505 (2013).

[24] F. Moučka, I. Nezbeda, and W. R. Smith, J. Chem. Theory Comput. **9**, 5076 (2013).

[25] P. T. Kiss and A. Baranyai, J. Chem. Phys. **141**, 114501 (2014).

[26] J. Kolafa, J. Chem. Phys. **145**, 204509 (2016).

[27] R. Elfgen, M. Hülsmann, A. Krämer, T. Köddermann, K. N. Kirschner, and D. Reith, Eur. Phys. J.: Spec. Top. **225**, 1391 (2016).

[28] I. Pethes, J. Mol. Liq. **242**, 845 (2017).

[29] H. J. C. Berendsen, J. P. M. Postma, W. F. Van Gunsteren, and J. Hermans, in *Intermolecular Forces*, edited by B. Pullman (Reidel Publishing Company, Dordrecht, 1981), p. 331.

[30] H. J. C. Berendsen, J. R. Grigera, and T. P. Straatsma, J. Phys. Chem. **91**, 6269 (1987).

[31] W. L. Jorgensen, J. Chandrasekhar, J. D. Madura, R. W. Impey, and M. L. Klein, J. Chem. Phys. **79**, 926 (1983).

[32] H. W. Horn, W. C. Swope, J. W. Pitera, J. D. Madura, T. J. Dick, G. L. Hura, and T. Head-Gordon, J. Chem. Phys. **120**, 9665 (2004).

[33] J. L. F. Abascal and C. Vega, J. Chem. Phys. **123**, 234505 (2005).

[34] J. Caldwell, L. X. Dang, and P. A. Kollman, J. Am. Chem. Soc. **112**, 9144 (1990).

[35] L. X. Dang, J. Chem. Phys. **97**, 2659 (1992).

[36] G. Lamoureux, A. D. MacKerell, Jr., and B. Roux, J. Chem. Phys. **119**, 5185 (2003).

[37] G. Lamoureux, E. Harder, I. V. Vorobyov, B. Roux, and A. D. MacKerell, Jr., Chem. Phys. Lett. **418**, 245 (2006).

[38] P. T. Kiss and A. Baranyai, J. Chem. Phys. **138**, 204507 (2013).

[39] I. Nezbeda, F. Moučka, and W. R. Smith, Mol. Phys. **114**, 1665 (2016).

[40] A. K. Mazur, J. Am. Chem. Soc. **125**, 7849 (2003).

[41] J. Alejandre, G. A. Chapela, F. Bresme, and J.-P. Hansen, J. Chem. Phys. **130**, 174505 (2009).

[42] F. Moučka, M. Lísal, and W. R. Smith, J. Phys. Chem. B **116**, 5468 (2012).

[43] F. Moučka, I. Nezbeda, and W. R. Smith, J. Chem. Phys. **138**, 154102 (2013).

[44] P. Auffinger, T. E. Cheatham, and A. C. Vaiana, J. Chem. Theory Comput. **3**, 1851 (2007).

[45] T. Martinek, E. Duboué-Dijon, Š. Timr, P. E. Mason, K. Baxová, H. E. Fischer, B. Schmidt, E. Pluhařová, and P. Jungwirth, J. Chem. Phys. **148**, 222813 (2018).

[46] E. Wernersson and P. Jungwirth, J. Chem. Theory Comput. **6**, 3233 (2010).

[47] E. Pluhařová, P. E. Mason, and P. Jungwirth, J. Phys. Chem. A **117**, 11766 (2013).

[48] M. Ferrario, G. Ciccotti, E. Spohr, T. Cartailler, and P. Turq, J. Chem. Phys. **117**, 4947 (2002).

[49] E. Sanz and C. Vega, J. Chem. Phys. **126**, 014507 (2007).

[50] A. S. Paluch, S. Jayaraman, J. K. Shah, and E. J. Maginn, J. Chem. Phys. **133**, 124504 (2010).

[51] F. Moučka, M. Lísal, J. Škvor, J. Jirsák, I. Nezbeda, and W. R. Smith, J. Phys. Chem. B **115**, 7849 (2011).

[52] J. L. Aragones, E. Sanz, and C. Vega, J. Chem. Phys. **136**, 244508 (2012).

[53] Z. Mester and A. Z. Panagiotopoulos, J. Chem. Phys. **143**, 044505 (2015).

[54] J. R. Espinosa, J. M. Young, H. Jiang, D. Gupta, C. Vega, E. Sanz, P. G. Debenedetti, and A. Z. Panagiotopoulos, J. Chem. Phys. **145**, 154111 (2016).

[55] A. L. Benavides, J. L. Aragones, and C. Vega, J. Chem. Phys. **144**, 124504 (2016).

[56] J. S. Kim, Z. Wu, A. R. Morrow, A. Yethiraj, and A. Yethiraj, J. Phys. Chem. B **116**, 12007 (2012).

[57] Z. Kann and J. Skinner, J. Chem. Phys. **141**, 104507 (2014).

[58] F. Moucka, I. Nezbeda, and W. R. Smith, J. Chem. Th. Comp. **11**, 1756 (2015).

[59] I. V. Leontyev and A. A. Stuchebrukhov, J. Chem. Phys. **130**, 085102 (2009).

[60] I. V. Leontyev and A. A. Stuchebrukhov, J. Chem. Theory Comput. **6**, 3153 (2010).

[61] I. V. Leontyev and A. A. Stuchebrukhov, J. Chem. Theory Comput. **6**, 1498 (2010).

[62] I. V. Leontyev and A. A. Stuchebrukhov, Phys. Chem. Chem. Phys. **13**, 2613 (2011).

[63] I. V. Leontyev and A. A. Stuchebrukhov, J. Chem. Theory Comput. **8**, 3207 (2012).

[64] I. V. Leontyev and A. A. Stuchebrukhov, J. Chem. Phys. **141**, 014103 (2014).

[65] Y. Yao, M. L. Berkowitz, and Y. Kanai, J. Chem. Phys. **143**, 241101 (2015).

[66] M. Kohagen, P. E. Mason, and P. Jungwirth, J. Phys. Chem. B **118**, 7902 (2014).

[67] M. Kohagen, P. E. Mason, and P. Jungwirth, J. Phys. Chem. B **120**, 1454 (2015).

[68] E. Duboué-Dijon, P. E. Mason, H. E. Fischer, and P. Jungwirth, J. Phys. Chem. B **122**, 3296 (2017).

[69] C. Vega, Mol. Phys. **113**, 1145 (2015).

[70] M. Jorge and L. Lue, J. Chem. Phys. **150**, 084108 (2019).

[71] A. W. Milne and M. Jorge, J. Chem. Theory Comput. **15**, 1065 (2018).

[72] A. L. Benavides, M. A. Portillo, V. C. Chamorro, J. R. Espinosa, J. L. F. Abascal, and C. Vega, J. Chem. Phys. **147**, 104501 (2017).

[73] J. Škvára and I. Nezbeda, Mol. Simul. **45**, 358 (2019).

[74] R. Fuentes-Azcatl and M. C. Barbosa, J. Phys. Chem. B **120**, 2460 (2016).

[75] J. Li and F. Wang, J. Chem. Phys. **143**, 194505 (2015).

[76] J. Li and F. Wang, J. Phys. Chem. B **121**, 6637 (2017).

[77] E. E. Bruce and N. F. van der Vegt, J. Chem. Phys. **148**, 222816 (2018).

[78] T. Sayer and S. J. Cox, Phys. Chem. Chem. Phys. **21**, 14546 (2019).

[79] C. Vega, J. L. F. Abascal, M. M. Conde, and J. L. Aragones, Faraday Discuss. **141**, 251 (2009).

[80] C. Vega and J. L. F. Abascal, Phys. Chem. Chem. Phys. **13**, 19663 (2011).

[81] H. Jiang, P. G. Debenedetti, and A. Z. Panagiotopoulos, J. Chem. Phys. **149**, 141102 (2019).

[82] A. L. Benavides, M. A. Portillo, J. L. F. Abascal, and C. Vega, Mol. Phys. **115**, 1301 (2017).

[83] W. M. Haynes, *CRC Handbook of Chemistry and Physics* (CRC Press, 2011).

[84] S. Pengsheng and Y. Yan, Calphad **27**, 343 (2003).

[85] E. Bock, Can. J. Chem. **39**, 1746 (1961).

[86] W. R. Cannon, B. M. Pettitt, and J. A. McCammon, J. Phys. Chem. **98**, 6225 (1994).

[87] B. Hess, C. Kutzner, D. van der Spoel, and E. Lindahl, J. Chem. Theory Comput. **4**, 435 (2008).

[88] U. Essmann, L. Perera, M. L. Berkowitz, T. Darden, H. Lee, and L. G. Pedersen, J. Chem. Phys. **103**, 8577 (1995).

[89] S. Nosé, Mol. Phys. **52**, 255 (1984).

[90] W. G. Hoover, Phys. Rev. A **31**, 1695 (1985).

[91] G. Bussi, D. Donadio, and M. Parrinello, J. Chem. Phys. **126**, 014101 (2007).

[92] M. Parrinello and A. Rahman, J. Appl. Phys. **52**, 7182 (1981).

[93] B. Hess, H. Bekker, H. J. C. Berendsen, and J. G. E. M. Fraaije, J. Comput. Chem. **18**, 1463 (1997).

[94] B. Hess, J. Chem. Theory Comput. **4**, 116 (2008).

[95] J. P. Ryckaert, G. Ciccotti, and H. J. Berendsen, J. Comput. Phys. **23**, 327 (1977).

[96] M. A. Gonzalez and J. L. F. Abascal, J. Chem. Phys. **132**, 096101 (2010).

[97] P. S. Z. Rogers and K. S. Pitzer, J. Phys. Chem. Ref. Data **11**, 15 (1982).

[98] K. S. Pitzer, J. C. Peiper, and R. Busey, J. Phys. Chem. Ref. Data **13**, 1 (1984).

[99] R. W. Potter and D. L. Brown, "The volumetric properties of aqueous sodium chloride solutions from O degrees to 500 degrees C at pressures up to 2000 bars based on a regression of available data in the literature," Technical Report 1421C, USGS, 1977.

[100] Y. Marcus, Chem. Rev. **88**, 1475 (1988).

[101] M. Laliberté, J. Chem. Eng. Data **52**, 321 (2007).

[102] M. Laliberté, J. Chem. Eng. Data **54**, 1725 (2009).

[103] Y. H. Li and S. Gregory, Geochim. Cosmochim. Acta **38**, 703 (1974).

[104] K. Müller and H. Hertz, J. Phys. Chem. **100**, 1256 (1996).

[105] I.-C. Yeh and G. Hummer, J. Phys. Chem. B **108**, 15873 (2004).

[106] G. H. Haggis, J. B. Hasted, and T. J. Buchanan, J. Chem. Phys. **20**, 1452 (1952).

[107] J. H. Christensen, A. J. Smith, R. B. Reed, and K. L. Elmore, J. Chem. Eng. Data **11**, 60 (1966).

[108] J. L. Aragones, M. Rovere, C. Vega, and P. Gallo, J. Phys. Chem. B **118**, 7680 (2014).

[109] M. Laliberte and W. E. Cooper, J. Chem. Eng. Data **49**, 1141 (2004).

[110] X. Zhang, P. Alvarez-Lloret, G. Chass, and D. Di Tommaso, Eur. J. Mineral. **31**, 275 (2019).

[111] S. Mao, Q. Peng, M. Wang, J. Hu, C. Peng, and J. Zhang, Appl. Geochem. **86**, 105 (2017).

[112] V. Vchirawongkwin, B. M. Rode, and I. Persson, J. Phys. Chem. B **111**, 4150 (2007).

[113] M. Duvail, A. Villard, T.-N. Nguyen, and J.-F. Dufreche, J. Phys. Chem. B **119**, 11184 (2015).

[114] H.-L. Zhang and S.-J. Han, J. Chem. Eng. Data **41**, 516 (1996).

[115] A. Campbell and E. Kartzmark, Can. J. Chem. **34**, 672 (1956).

[116] H.-L. Zhang, G.-H. Chen, and S. J. Han, J. Chem. Eng. Data **42**, 526 (1997).

[117] D. Zezin, T. Driesner, S. Scott, C. Sanchez-Valle, and T. Wagner, J. Chem. Eng. Data **59**, 2570 (2014).

[118] D. Zezin, T. Driesner, and C. Sanchez-Valle, J. Chem. Eng. Data **60**, 1181 (2015).

[119] S. Yue and A. Z. Panagiotopoulos, "Dynamic properties of aqueous electrolyte solutions from non-polarisable, polarisable, and scaled-charge models," Molec. Phys. (published online).

[120] D. Laage and G. Stirnemann, J. Phys. Chem. B **123**, 3312 (2019).